Extremophiles (2003) 7:145–157
DOI 10.1007/s00792-002-0306-3

ORIGINAL PAPER

Marianne Brugna-Guiral · Pascale Tron
Wolfgang Nitschke · Karl-Otto Stetter
Benedicte Burlat · Bruno Guigliarelli
Mireille Bruschi · Marie Thérèse Giudici-Orticoni

[NiFe] hydrogenases from the hyperthermophilic bacterium *Aquifex aeolicus*: properties, function, and phylogenetics

Received: 17 July 2002 / Accepted: 7 November 2002 / Published online: 23 January 2003

Abstract Genes potentially coding for three distinct [NiFe] hydrogenases are present in the genome of *Aquifex aeolicus*. We have demonstrated that all three hydrogenases are expressed under standard growth conditions of the organism. Two hydrogenases were further purified to homogeneity. A periplasmically oriented hydrogenase was obtained in two forms, i.e., as a soluble enzyme containing only the two essential subunits and as a detergent-solubilized complex additionally containing a membrane-integral *b*-type cytochrome. The second hydrogenase purified was identified as a soluble cytoplasmic enzyme. The isolated enzymes were characterized with respect to biochemical/biophysical parameters, activity, thermostability, and substrate specificity. The phylogenetic positioning of all three hydrogenases was analyzed. A model for the metabolic roles of the three enzymes is proposed on the basis of the obtained results.

Keywords *Aquifex aeolicus* · Hydrogenase · Phylogeny · Hydrogen metabolism

Introduction

Microorganisms having the remarkable property of growing at temperatures near and above 100 °C have been isolated from shallow submarine and deep-sea volcanic environments over the last 20 years (Adams 1994; Stetter 1996, 1999). The majority of these hyperthermophilic microorganisms belongs to the domain of the Archaea and is considered to represent the most slowly evolving forms of life (Adams 1994; Stetter 1996, 1999). The discovery of hyperthermophiles has important ramifications, not only in microbial physiology and evolution but also in biotechnology (Kelly and Adams 1994). Whereas numerous hyperthermophilic Archaea are known, only very few hyperthermophilic organisms from the domain of the Bacteria have been discovered so far. The most hyperthermophilic Bacteria known to date are members of the genus *Aquifex* (Huber et al. 2000; Huber and Stetter 2001). According to phylogenetic trees based on small subunit rRNA, the Aquificales represent the earliest branching order of the domain Bacteria (Olsen 1994). Aquificales typically are thermo- or hyperthermophilic, hydrogen-oxidizing, microaerophilic, obligate chemolithoautotrophs (Huber et al. 2000; Huber and Stetter 2001). The genome of a hyperthermophilic representative, *Aquifex aeolicus*, was sequenced a few years ago (Deckert et al. 1998).

Stimulated by the exceptional phylogenetic and physiological properties of *A. aeolicus*, as well as by its potential as a source of extremely thermostable enzymes, we have set out to study the hydrogen metabolism of this organism. Hydrogenases play a key role in this process. These enzymes were first isolated from prokaryotes of the domain Bacteria (Adams 1990) and subsequently from Archaea (Adams and Kelly 1998). Hydrogenases have also been found in subcellular organelles of eukaryotes and in chloroplasts of green algae. Depending on the metabolic requirements of the parent organism, hydrogenases catalyze either the hydrogen uptake or the hydrogen evolution half of the reversible reaction $H_2 \Leftrightarrow 2H^+ + 2e^-$. The majority of hydrogenases are metalloenzymes and are classed in two main categories according to the nature of their catalytic sites (Adams 1990; Vignais et al. 2001). The so-called iron-only

Communicated by A. Driessen

M. Brugna-Guiral · P. Tron · W. Nitschke · B. Burlat
B. Guigliarelli · M. Bruschi · M.T. Giudici-Orticoni (✉)
Bioénergétique et Ingénierie des Protéines, CNRS, IBSM,
31 chemin Joseph Aiguier, 13402 Marseille Cedex 20, France
E-mail: giudici@ibsm.cnrs-mrs.fr
Tel.: +33-4-91164550
Fax: +33-4-91164578

K.-O. Stetter
Lehrstuhl für Mikrobiologie,
Universität Regensburg, Regensburg, Germany

hydrogenases have high specific activities but are strongly oxygen-labile, whereas the [NiFe] hydrogenases, less active than [Fe] hydrogenases, are more resistant to O_2.

Hydrogenases have been detected in the cytoplasm and in the periplasm or have been associated with the membrane in the various species studied. For several of these organisms, the presence of more than one hydrogenase has been described (Fauque et al. 1988; Friedrich and Schwartz 1993; Voordouw 1993). The functional role of hydrogenases has been studied in aerobic and anaerobic respiratory systems, and most of the data gathered so far have been obtained on eubacterial systems. In aerobic H_2-oxidizing prokaryotes, [NiFe] hydrogenases can function both as cytoplasmic NAD-reducing enzymes and as a part of conventional membrane-bound respiratory chains where O_2 is the terminal acceptor (Albracht 1993). In contrast, in anaerobic respiratory systems, the role of hydrogenases is less well understood. Sequence alignments have been used by Wu and Mandrand (1993) and more recently by Vignais et al. (2001) to define four groups of [NiFe] hydrogenases. Group 1 hydrogenases transfer electrons from hydrogen to membrane-integral cytochrome, coupling electron transfer with transmembrane proton translocation. This group also includes the periplasmic soluble hydrogenases from sulfate-reducing bacteria. Group 2 comprises the cyanobacterial uptake hydrogenases and the cytoplasmic soluble hydrogenases involved in hydrogen sensing. The heterotetrameric [NiFe] hydrogenases of group 3 contain additional subunits able to bind soluble cofactors such as factor F_{420}, NAD, or NADP. Group 4 contains the membrane-associated, hydrogen-evolving respiratory [NiFe] hydrogenases.

The annotation of the *A. aeolicus* genome suggests the presence of as much as three operons potentially encoding distinct [NiFe] hydrogenases (in the following, referred to as hydrogenases I, II, and III in keeping with the annotated names mbhSL1, mbhSL2, and mbhSL3). This possible multitude of different hydrogenases adds to the interest of studying the components of hydrogen metabolism in *A. aeolicus*. Some of these enzymes may be isoforms expressed under varying growth conditions, whereas others may perform significantly differing metabolic functions.

In this work, we report the purification as well as the biochemical and biophysical characterization of two soluble hydrogenases and one membrane-attached [NiFe] hydrogenase. The latter enzyme was found to contain *b*-type cytochrome. N-terminal sequencing identified the purified enzymes as the gene products of the [NiFe] hydrogenases I and III detected in the genome. Hydrogenase II was seen to be present in crude extracts. Observed physicochemical parameters and possible metabolic roles are discussed on the basis of information provided by the amino acid sequences and the analysis of the phylogenetic positioning of the respective enzymes.

Materials and methods

Organism and growth conditions

Aquifex aeolicus was cultivated and harvested as described previously (Deckert 1998).

Enzyme purification

Hydrogenases from *A. aeolicus* were purified at room temperature. All buffers were pre-incubated under argon to remove any oxygen traces. Cell material (50 g) was resuspended in Hepes/NaOH 50 mM pH 7, 4 mM EDTA, 0.5 mM PMSF (buffer A), and DNAse I 10 μg/ml and broken in a French Press at 18–20 kpsi. Unbroken cells and debris were removed by centrifugation at 10,000 *g* for 15 min. Membranes were collected by centrifugation at 200,000 *g* for 1 h. Soluble hydrogenase was purified from the supernatant fraction. The supernatant was loaded on a DEAE cellulose column (2×10 cm) equilibrated with buffer A. The adsorbed proteins were eluted by a nonlinear gradient of NaCl (50–500 mM) in the same buffer. Two fractions containing hydrogenase activity eluted at 50 mM (A) and at 150–200 mM (B) salt concentration. Each fraction was loaded onto a hydroxylapatite Bio-GelHTP column (1.5×8.5 cm) equilibrated in buffer A, 50 mM NaCl, or buffer A, 200 mM NaCl. The hydrogenase fraction A eluted at 50 mM phosphate, and the hydrogenase fraction B eluted at 200 mM phosphate. The samples were concentrated using a centriprep PM 30 (Amicon) and stored in liquid N_2 in the presence of 10% glycerol. Membrane fragments were resuspended to a protein concentration of 10 mg/ml in buffer A. *n*-Dodecyl-*β*-D-maltoside (DDM) (1.5 mg/mg of protein) was added and the membrane proteins were extracted while stirring for 1 h at 25 °C under argon. The resulting suspension was centrifuged at 200,000 *g* for 1 h, and the resulting supernatant was concentrated and loaded onto a sucrose density gradient (20% to 50% in buffer A plus DDM 0.05%). After dialysis, the hydrogenase activity-containing fraction M (recovered at 25–30% sucrose) was loaded onto a DEAE cellulose column (4.5×9.5 cm) equilibrated in buffer A, DDM 0.05%. The fraction eluting at 150 mM NaCl and containing the hydrogenase activity was loaded onto a hydroxyapatite column equilibrated in Tris-HCl 50 mM pH 7, NaCl 150 mM, DDM 0.05%. The protein eluted when 400 mM phosphate was applied to the column. After dialysis, the hydrogenase fraction was loaded onto a column Mono Q (FPLC apparatus, Amersham Pharmacia Biotech) equilibrated with buffer A, DDM 0.05%, at a flow rate of 1 ml/min. Proteins were eluted by a linear gradient from 0 to 500 mM NaCl. Fractions containing hydrogenase M activity eluted at 120 mM in NaCl and were concentrated and stored in liquid N_2 in the presence of 10% glycerol.

Hydrogenase activity assays

Hydrogenase activity was routinely determined at 80 °C by the hydrogen consumption assay, using methylviologen as the electron acceptor and hydrogen as the electron donor. The hydrogen-dependent reduction rate of methylviologen was followed spectrophotometrically at 604 nm ($\epsilon_{604} = 13600\ M^{-1}\ cm^{-1}$). All assays were done at 80 °C in 50 mM HEPES buffer pH 7, 1 mM methylviologen. Prior to the experiment, the cuvette was first bubbled with argon (10 min), then with hydrogen gas (10 min) and subsequently incubated at 80 °C (10 min). At time zero, the reaction was started by addition of an appropriate amount of enzyme previously incubated at 80 °C (10 min). H_2 production assay was determined using reduced methylviologen as electron donor and was followed spectrophotometrically at 604 nm.

The standard assay mixture without methylviologen was furthermore used to assay for reduction of alternative electron acceptors by the soluble hydrogenase. The following extinction

coefficients (mM^{-1} cm^{-1}) were used: methylene blue, 32.8 at 600 nm; phenazine methosulfate, 23.8 at 387 nm; DCIP, 20.6 at 600 nm; ferricyanide, 1.04 at 420 nm.; NAD/NADH, 6.3 at 340 nm; and NADP/NADPH, 6.3 at 340 nm.

One unit of enzyme activity is defined as the amount of enzyme required for the reduction of 2 μmol of methylviologen per min in the presence of excess hydrogen. The specific activity is defined as the number of enzymatic units per mg of protein.

The pyruvate oxidation activity of PFOR was assayed by monitoring the pyruvate- and CoA-dependent reduction of methylviologen under anaerobic conditions at 80 °C as described in Blamey and Adams (1993).

Temperature dependence and thermal stability

The temperature dependence of the enzyme activity was measured between 20 °C and 100 °C in 50 mM Hepes, pH 7. Thermodynamic parameters for the rate-determining step were obtained from the Arrhenius plot for hydrogenase activity.

$$\ln(k) = \ln A - Ea/RT$$

where Ea is the activation energy, A is the intercept of the Arrhenius equation, R is the gas constant, and T is the absolute temperature (Segel 1993).

The thermostability of the purified enzyme was tested in sealed vials, which were incubated at 80 °C for up to 120 min. The vials were then cooled on ice for 5 min, and the remaining enzyme activity was tested at 80 °C.

Analytical procedures

Electrophoreses were carried out under native or reducing conditions on a Pharmacia Phast System with Phast Gels 12% polyacrylamide and Phast Gel native or SDS buffer strips.

The samples were stained with Coomassie blue. Hydrogenase activity was revealed on the gel by incubating the native gel first in degassed 50 mM HEPES pH 7 then in 2 mM methylviologen in Hepes buffer saturated with argon then with hydrogen and finally raising the temperature to 80 °C for 15 min; 1 mM triphenyltetrazolium chloride fixed the red coloration of the bands corresponding to hydrogenase (Ackrell et al. 1966). After electrophoresis under denaturing conditions, the proteins were transferred onto nitrocellulose membranes (Pharmacia). Immunodetection was performed with rabbit anti-*Desulfovibrio fructosovorans* [NiFe] hydrogenase antiserum (Sambrook et al. 1989).

Proteomic experiments

Two-dimensional electrophoreses were performed on a Multiphor II Electrophoresis System (Pharmacia). The first dimension run was done with immobiline DryStrip gels (180×3 mm) and pH range (3–10). The hydrogenase activity was revealed as previously described without fixation with triphenyltetrazolium. The run in the second-dimension run was carried out under reducing conditions on 10% SDS-PAGE.

The N-terminal amino acid sequence of the hydrogenase subunits was determined from the enzyme preparation after separation of the subunits by SDS-PAGE. After electrophoresis on a 10% polyacrylamide gel under denaturing conditions, proteins were transferred onto a polyvinylidene difluoride (PVDF) membrane for 40 min at a current intensity of 0.8 mA/cm^2 using a semi-dry electrophoretic transfer unit. Sequence determinations were carried out with an Applied Biosystems A470 gas-phase sequenator. Quantitative determination of phenylthiohydantoin derivatives was done by high-pressure liquid chromatography (Water Associates, Inc) monitored by a data and chromatography control station (Waters 840).

Membranes were solubilized with dodecylmaltoside. The solubilized fraction was analyzed by native PAGE. The hydrogenase activity was detected as previously described. Digestion of excised gel plugs (in-gel) was performed as described in Jensen et al. (1998). The excised gel plugs were proteolyzed in situ by trypsin using the following procedure. The band was first washed with H_2O, 100 mM NH_4HCO3, then CH_3CN (3 times). Second step: reductive alkylation, 10 mM DTT in 100 mM NH_4HCO3, for 45 min at 56 °C, then 55 mM Iodoacetamine in 100 mM NH_4HCO3 for 30 min at 25 °C, and finally 100 mM NH_4HCO3, for 5 min and CH_3CN for 5 min. Proteolysis: the band was incubated in trypsin (Promega) 12.5 ng/μl in 25 mM NH_4HCO3 for 45 min then washed overnight in 25 mM NH_4HCO3. The supernatant was desalted and the analysis of the peptides was performed on MALDI-TOF Voyager DE-RP (Perceptice). Protein identification by mass spectrometry data was accomplished using NCBI's nr (All non-reductant GenBank CDS translations + PDB + SwissProt + PIR + PRF) database (http://prowl.rockefeller.edu/cgi-bin/ProFound).

Protein concentrations were measured by the Bradford method using bovine serum albumin as standard (Bradford 1976).

Electron paramagnetic resonance spectroscopy

Electron paramagnetic resonance (EPR) spectra were recorded on a Bruker ER300e X-band spectrometer fitted with an Oxford Instruments liquid He cryostat. Oriented membrane multi-layers were produced according to Blasie et al. (1978) and Rutherford and Sétif (1990).

Sequence and phylogenetic analysis

Multiple sequence alignments were performed using ClustalX (Altschul et al. 1990), and prediction of secondary structure was carried out using the pSAAM package for Windows, a program for protein sequence analysis and modeling (University of Illinois). In places, the multiple alignment arrived at by ClustalX was optimized by hand based on results of secondary structure prediction. Phylogenetic relationships were calculated using the neighbor-joining approach (ClustalX) of Saitou and Nei, as well as Kimura's correction for multiple substitutions. Gap positions were excluded. Bootstrap values indicated in phylograms correspond to the frequency of occurrence of nodes in 1,000 bootstrap replicates. Sequences were retrieved via the NCBI server (http://www.ncbi.nlm.nih.gov/).

Results

Identification of three hydrogenases in *Aquifex aeolicus* by proteomic analysis

After ultracentrifugation of broken cells, hydrogenase activity was observed in both the supernatant and the membrane fraction (20% activity in the supernatant vs 80% in the pellet). Identification of hydrogenase was performed by gel electrophoresis, mass spectrometry, and bioinformatics. The first-dimension electrophoresis (isoelectric focusing) of the two fractions clearly shows two bands of activity in the membrane fraction with isoelectric points of 6.5 and 7, respectively, and one major band in the soluble fraction with an isoelectric point of 6.2. The second dimension in SDS-PAGE and the transfer on PVDF allowed us to determine the corresponding N-terminal sequences. In the soluble fraction, the N-terminal sequences of the small (MKLL...)

and the large (MKIEKL...) subunits of hydrogenase III as predicted by the genome were obtained. In the membrane fraction, where two bands with hydrogenase activity were present, the determined N-terminal sequences identified the large (MKRVV...) and the small (METKP...) subunits of hydrogenase I. The presence of hydrogenase II could not be demonstrated at this stage.

After native electrophoresis of the membrane fraction, the two bands showing hydrogenase activity were proteolyzed in situ by trypsin. The peptides obtained were analyzed by mass spectrometry. The peptide maps produced by mass spectrometry allowed identification of proteins relative to full-length protein sequence information derived from the genome. The obtained data were matched against all bacterial and archaeal proteins in NCBI's protein nr or SWISS-protein nr database, using a pI range of 4–8 and a mass range of 50–200 kDa. For the first band, the sequence coverage was 46%, 27%, and 33% for the large and the small subunit of hydrogenase I as well as cytochrome *b* encoded by the gene *hoxZ*, respectively. Hydrogenase II was identified in the same way with a sequence coverage of 27% and 50% for the small and large subunit, respectively.

Purification of hydrogenases

The two hydrogenases A and B responsible for the activity in the soluble extract were purified. For hydrogenase A, one band was observed when the enriched hydrogenase sample was run on native PAGE and stained for activity. Two bands of 40 and 70 kDa were revealed by SDS-PAGE (Fig. 1, lane 2), and the N-terminal sequences of the two subunits were determined after transfer onto a PVDF membrane. The sequences for the large and small subunits are MKRVV and METKPRV, respectively. These sequences correspond to the N-terminal sequences of the large and small subunits of hydrogenase I. Purified hydrogenase I had a UV-visible absorption spectrum typical of an iron-sulfur protein with an A390/A280 of 0.36. Three milligrams of pure enzyme with a specific activity of 4U/mg at 80 °C in H_2 oxidation was obtained.

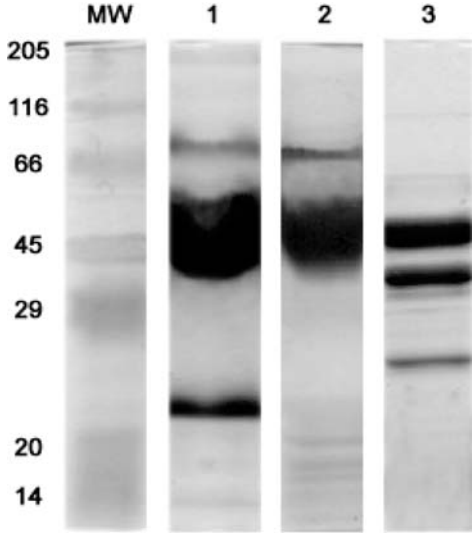

Fig. 1 SDS-PAGE of the purified *Aquifex aeolicus* hydrogenases. *MW* Molecular mass marker, *lane 1* hydrogenase I–cytochrome *b* complex, *lane 2* hydrogenase I alone, *lane 3* hydrogenase III

For hydrogenase B also one band was observed when the enriched hydrogenase sample was run on native PAGE and stained for activity. Two bands of 30 and 50 kDa were revealed on SDS-PAGE (Fig. 1, lane 3) and by Western blotting (not shown). The N-terminal sequences of the two subunits were again determined after transfer onto a PVDF membrane. The sequences for the large and small subunits are MKIEKL and MKLLWL, respectively. These sequences correspond to the N-terminal sequences of the large and small subunits of hydrogenase III. Purified hydrogenase III had a UV-visible absorption spectrum typical of an iron-sulfur protein with an A390/A280 of 0.26. The pure enzyme (3.5 mg) had a specific activity of 100 U/mg at 80 °C in the H_2 oxidation. Freshly prepared hydrogenase III in the absence of glycerol is highly unstable. At both 20 °C and 80 °C, the activity decayed very rapidly in the first few days of storage in the absence of glycerol under argon. However, including 10% glycerol in the storage medium strongly diminished inactivation.

Hydrogenase M (4.5 mg) obtained from the membrane fraction was identified as a hydrogenase I–cytochrome *b* complex by MALDI-TOF Voyager DE-RP and by SDS-PAGE where three bands of 70, 40, and 20 kDa were revealed (Fig. 1, lane 1). The UV-visible absorption spectra showed a Soret peak at 418 nm in the oxidized state and peaks at 430–435 nm (Soret), 525–530 nm, and 560 nm in the reduced state (Fig. 2). Addition of ascorbate reduced the total heme by 60%, yielding a Soret peak at 429 nm (dashed line). Full reduction was achieved by addition of dithionite or H_2. The Soret peak of the additionally reduced heme (Fig. 2, continuous line) was found to be shifted to 433 nm, demonstrating the presence of at least two distinct hemes with distinguishable redox midpoint potentials. The EPR spectrum of fully oxidized hydrogenase M was characterized by a dominant low-spin g_z-peak at $g = 3.2$ (Fig. 2, inset). The g_z-peak at $g = 2.9$ was substoichiometric and therefore most probably represents a degraded fraction of the cytochrome.

The enzyme had a specific activity of 13 U/mg at 80 °C in H_2 oxidation. As compared to the cell extract, the activity yield was 26% for the soluble hydrogenase I, 9% for the soluble hydrogenase III, and 7% for the hydrogenase I–cytochrome *b* complex.

EPR characterization of the soluble form of hydrogenases I and III

After purification, a freshly prepared solution of hydrogenase III was oxidized by addition of 2 equivalents

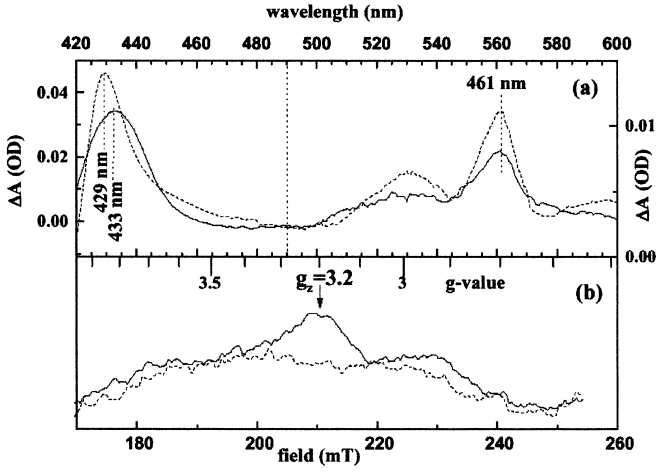

Fig. 2 a Absorption difference spectra (ascorbate-reduced minus oxidized, *dashed line*; dithionite-reduced minus ascorbate-reduced, *continuous line*) of purified hydrogenase I–cytochrome *b* complex. **b** EPR spectra of hydrogenase I–cytochrome *b* complex in the region of low-spin heme signals recorded on fully oxidized (*continuous line*) and H2-reduced (*dashed line*) samples. EPR conditions: microwave frequency, 9.42 GHz; microwave power; 6.3 mW; modulation amplitude, 3.2 mT; temperature, 15 K

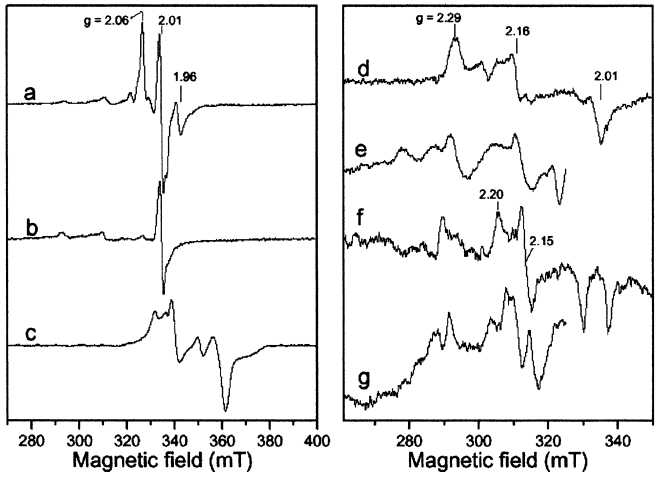

Fig. 3 Hydrogenase III EPR spectra given by [Fe-S] centers (left panel) and [Ni-Fe] center (right panel). *a*, *d*, *e* DCIP oxidized enzyme. *b* Ascorbate-reduced enzyme. Enzyme reduced by hydrogen (*f*, *g*) and dithionite (*c*). Experimental conditions: temperature, 15 K (*a*, *b*), 6 K (*c*, *e*, *g*), 70 K (*d*, *f*); modulation amplitude, 1 mT at 100 kHz; microwave power at 9.419 GHz, 1mW (*a*, *b*), 10 mW (*c*–*g*). For sake of clarity, iron-sulfur cluster contribution was not shown on traces *e* and *g*

of dichloroindophenol (DCIP). This treatment enabled us to fully oxidize the enzyme, since it led to an EPR spectrum that does not change upon further addition of DCIP or a stronger oxidant like potassium hexachloroiridate (IV) (E_m1.02 V). At 15 K, this spectrum is composed of a complex signal in the $g = 2.0$ region, with major features at $g = 2.06$, 2.01, and 1.96, and of weaker lines at $g = 2.29$ and 2.16 (Fig. 3a). The complex signal disappears by relaxation broadening for temperatures higher than 70 K, which indicates that it arises from rapidly relaxing iron-sulfur clusters. In contrast, the other lines are well visible at this temperature and reveal a rhombic signal at $g = 2.29$, 2.16, and 2.01, which likely corresponds to the Ni-B state of the [Ni-Fe] center of the enzyme (Fig. 3d). No Ni-A signal was observed, which shows that the oxidized enzyme is entirely in the so-called "ready form" that can be rapidly activated upon reduction (Albracht 1993). Below about 8 K, the Ni-B signal shows strong changes due to magnetic coupling of the [Ni-Fe] center with another paramagnetic species (Fig. 3e).

Upon mild reduction of the enzyme by 2 equivalents of sodium ascorbate, the complex signal in the $g = 2.0$ region disappeared and was replaced with a nearly isotropic signal at $g = 2.01$, which arises from the oxidized $[3Fe\text{-}4S]^{1+}$ cluster (Fig. 3b), and, concomitantly, the Ni-B lines became sharper. Such a behavior also was previously observed in [Ni-Fe] hydrogenases from *Chromatium vinosum* and *Thiocapsa roseopersicina* (Cammack et al. 1989; Surerus et al. 1994). It was interpreted as resulting from a magnetic coupling between the [Ni-Fe] center and the $[3Fe\text{-}4S]^{1+}$ cluster mediated by an intermediate paramagnetic species. This species would become diamagnetic upon reduction, inducing the uncoupling of the two centers (Surerus et al. 1994). To date, attempts to identify this intermediate species, metal ion, or radical species have been unsuccessful.

A further reduction of the hydrogenase III sample by incubation under H_2 atmosphere for 30 min at room temperature led to the disappearance of the Ni-B and $[3Fe\text{-}4S]^{1+}$ EPR signals. The Ni-B spectrum was replaced with the Ni-C spectrum at $g = 2.20$, 2.15, and 2.01 (Fig. 3f), corresponding to the active form of the enzyme. In addition, another unreported Ni signal could be observed at $g = 2.32$ and 2.04 and probably corresponds to a denatured fraction of the enzyme. At very low temperature, these Ni signals are split by the magnetic interaction with the reduced proximal [4Fe-4S] cluster (Fig. 3g). Moreover, the reduction of the [4Fe-4S] centers of the enzyme led to a complex signal visible in the range $g = 2.06$–1.75 (Fig. 3c) and likely arising from inter-cluster spin-spin coupling. Interestingly, this interaction signal has sharper lines and is much more resolved than those observed in other reduced [Ni-Fe] hydrogenases (Guigliarelli et al. 1995). This may reflect differences in the magnetic parameters or in the relative arrangement of the $[4Fe\text{-}4S]^{1+}$ clusters of hydrogenase III in comparison with other [Ni-Fe] enzymes (Guigliarelli et al. 1995). These EPR signal were not modified by an additional incubation of the enzyme under H_2 atmosphere for 30 min at 80 °C, but a further reduction by dithionite led to the disappearance of the Ni signals (Fig. 3c).

Similar experiments were carried out on soluble preparation of hydrogenase I and gave essentially the same EPR spectra, showing that the nature and the organization of the metal centers are comparable in the two enzymes.

Molecular and catalytic properties of hydrogenases from *A. aeolicus*

The purified enzymes were active in a large range of temperatures (20–90 °C) and did not need activation. This is consistent with the presence of the Ni-B species alone in the oxidized state of the purified enzymes. For all the enzymes isolated, we have observed a diminishing of the lag time in kinetic assays correlated with rising temperatures. This result suggests that the presence of an active form of the enzyme is favored at high temperatures. Hydrogenase III, hydrogenase I, and hydrogenase complexed with cytochrome *b* showed a temperature optimum of 80 °C. The activation energies were calculated from the Arrhenius plot. For hydrogenase I alone, the determination of the activation energy revealed that the enzyme exhibited a biphasic or discontinuous Arrhenius plot with two characteristic energies of activation (44 and 64 kJ/mol) and a break point at 64 °C. Such biphasicity in the energy of activation for the hydrogenase has not been reported so far. Discontinuous Arrhenius plots have been observed in membrane proteins (Charnock et al. 1971) and for certain enzymes from thermophiles (Amutha et al. 1998; Spies et al. 2000). The break in the Arrhenius plot may be explained by the existence of two conformational states of the enzyme above and below the break point, each with a different catalytic competence (Segel 1993). By contrast, the hydrogenase I–cytochrome *b* complex and hydrogenase III yielded monophasic Arrhenius plots with activation energies of 94 kJ/mol and 50 kJ/mol, respectively. As described in Materials and Methods, the thermodynamic parameters for the rate-determining step were calculated from the Arrhenius plot. The hydrogenase I–cytochrome *b* complex therefore is characterized by a higher activation energy than hydrogenase I alone or hydrogenase III. The minimum energy required for the reaction to occur is greater in the complex than in the cytochrome-free enzyme. This may be rationalized by a greater rigidity of the membrane complex as compared to the soluble hydrogenase.

The temperature stability of all hydrogenases was tested at 80 °C in 50 mM Hepes by incubating the enzyme in the absence of O_2 for up to 120 min. Hydrogenase III and the hydrogenase I–cytochrome *b* complex showed high stability against thermal inactivation (up to 4 h for the hydrogenase I–cytochrome *b* complex) under these conditions (up to 85%of activity was conserved). In contrast, hydrogenase I alone was very unstable and the activity was totally lost after 120 min. An alteration in thermostability has already been demonstrated for purified hydrogenase of hyperthermophilic Archaea compared to the same enzyme associated to the membrane. The latter complex was more resistant to high temperatures (Pihl and Maier 1991; Sapra et al. 2000) due to the hydrophobic interactions between the membrane and the hydrogenase, resulting in the stabilization of the whole structure. In our case, interaction between hydrogenase I and cytochrome *b* may also explain the higher stability as compared to hydrogenase alone.

The hydrogenase I–cytochrome *b* complex was found to be very sensitive to O_2. Exposure to 20% O_2 for 30 min at 0 °C resulted in loss of activity. A comparable result was observed on hydrogenase III only after 1.5 h. This sensitivity to oxygen may explain the significant loss of activity observed during the purification steps. In contrast, hydrogenase I in the absence of cytochrome *b* appears to be rather tolerant to oxygen, since 50% of the initial activity was still measured after exposure to O_2 for 24 h. Temperature experiments have shown that hydrogenase I probably was purified in an inactive (or less active) form that appears to be less sensitive to oxygen. This may also explain the better yield in the purification of this enzyme. Such an inactivated fraction of the enzyme could explain the presence of the unusual Ni EPR signal observed in addition to the Ni-C spectrum in the H_2-reduced state of the enzyme. This finding contrasts to results obtained on other hyperthermostable hydrogenases purified from membranes (Sapra et al. 2000). The difference may be due to the purification protocol.

All hydrogenases purified from *A. aeolicus* were inhibited by CO. This result is in contrast with those obtained with tetrameric hydrogenases from other hyperthermophilic organisms such as *Pyrococcus* (Bryant and Adams 1989; Ma et al. 2000). In these organisms the hydrogenases are able to reduced S° to H_2S (Ma et al. 2000). This difference could be explained by the dimeric structure of the hydrogenases from *Aquifex*.

Hydrogenases from *A. aeolicus* can couple H_2 uptake with the reduction of electron acceptors in a wide range of redox potentials (Table 1). The abilities to use these acceptors are comparable for hydrogenase I alone and the hydrogenase I–cytochrome *b* complex. As for all hydrogenases in this class, the reduction of electron acceptors with a positive redox midpoint potential was more efficient than the reduction of low-potential electron acceptors (Dross et al. 1992; Bernhard et al. 1997). The reduction of acceptors with low redox potential was more efficient with hydrogenase III. This finding is indicative of significant differences in the E_m values of the

Table 1 Comparison of hydrogenase III, hydrogenase I, and hydrogenase I–cyt *b* complex for ability to couple H_2 oxidation to various electron acceptors

Electron acceptor	E_m (mV)	Relative activity (%)		
		Hydrogenase III	Hydrogenase I	Hydrogenase I–cyt *b*
Methyl viologen	−446	100	23	18
Methylene blue	11	100	100	100
Phenazine methosulfate	80	3	11	0
DCIP	217	4	1.5	6

internal electron transfer chain (the three iron sulfur centers located on the small subunit, see below) between hydrogenase I and hydrogenase III. Consequently, the equilibrium of the catalytic reaction was less in favor of H_2 oxidation in hydrogenase III (ratio of 2) than in hydrogenase I (ratio of 0.3).

None of these hydrogenases catalyzed the H_2-dependent reduction of NAD or NADP, and no H_2 evolution activity could be detected by using NADPH or NADH as electron donors.

Sequence analysis

The large subunit

The large subunit of [NiFe] hydrogenases harbors the catalytic site, i.e., the [NiFe] center ligated by four cysteine residues which fall into two pairs at the N- and C-terminal ends of the protein. The respective pairs are surrounded by reasonably well-conserved sequence stretches termed the L1 (N-terminal) and L2 (C-terminal) motifs. Classification of hydrogenases into four distinct groups is based mainly on the presence or absence of specific residues within the L1 and L2 motifs (Vignais et al. 2001). The four cysteine residues are fully conserved in appropriate sequence positions in all three hydrogenases from *A. aeolicus*. Accordingly, the EPR characteristics of the [NiFe] center obtained on hydrogenases I and III (Fig. 3) strongly resemble those of other enzymes characterized.

The L1 and L2 motifs found in hydrogenases I and II perfectly fit the criteria for group 1 hydrogenases. By contrast, the respective motifs in hydrogenase III do not fall into any of the four major groups of [NiFe] hydrogenases (Vignais et al. 2001; see also Phylogeny below).

The small subunit

The so-called small subunit of typical [NiFe] hydrogenases has a two-domain structure (Volbeda et al. 1995). The N-terminal domain is common to all groups of [NiFe] hydrogenases and ligates the proximal [Fe-S] cluster, i.e., the [4Fe-4S] center that is in close proximity to the catalytic site on the large subunit. The C-terminal domain, by contrast, is variable among the different groups. The crystal structures of the [NiFe] and [NiFeSe] hydrogenases from *Desulfovibrio gigas* and *Desulfomicrobium baculatum*, respectively, show that in these species the C-terminal domain harbors two further [Fe-S] clusters that form, together with the proximal cluster, a roughly linear chain of redox centers extending from the surface of the enzyme towards the catalytic site deeply buried within the heterodimeric enzyme. Cluster-ligating residues are indicated in the sequence alignment shown in Fig. 4. The intermediate cluster is a [3Fe-4S] center in the *Desulfovibrio gigas* [NiFe] enzyme, whereas it is a [4Fe-4S] center in the *Desulfomicrobium baculatum* [NiFeSe] hydrogenase. The additional cysteine residue providing the fourth cluster ligand is marked in Fig. 4. The distal cluster is a noteworthy exception to the "all-cysteine" rule for [Fe-S] centers since it contains a histidine ligand

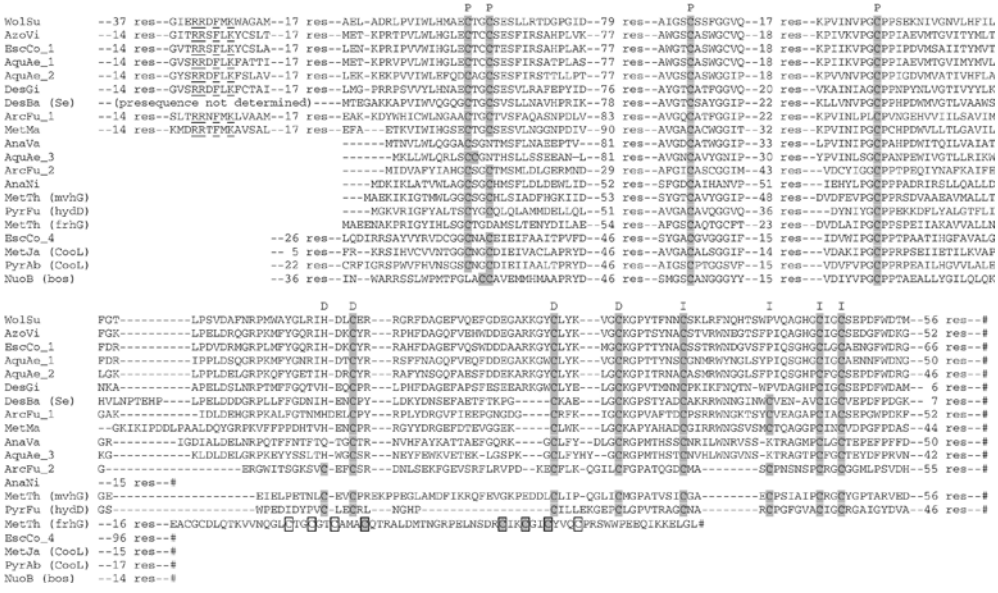

Fig. 4 Multiple sequence alignment of the small subunits from [NiFe] hydrogenase covering representatives from all four major groups as defined by Wu and Mandrand (1993). The first and second blocks correspond to the N- and C-terminal domains of the small subunit, respectively. The tat-signal sequence is indicated by *underscored* residues. Cluster-binding cysteine residues are marked by *gray shading*, and the histidine ligand to the distal cluster is highlighted in *bold*. Ligands to individual clusters are identified by *P* (proximal), *I* (intermediate), and *D* (distal). The ligands to the clusters in the C-terminal ferredoxin domain of the *frhG* gene product in *Methanobacterium thermoautotrophicum* are *boxed*. Abbreviations of species names are as indicated in the legend to Fig. 5

situated close to the surface of the small subunit (Volbeda et al. 1995). As indicated by the sequence alignment, the C-terminal domain can be replaced by a domain showing characteristic features of "bacterial-type" [8Fe-8S] ferredoxins or, alternatively, can be completely absent.

The sequence features of hydrogenases I and II from *Aquifex aeolicus* are strongly homologous to those of the enzyme from *Desulfovibrio gigas* for which the 3-D structure is available. In particular, the absence of a fourth ligand to the intermediate cluster as well as the conservation of the histidine residue serving as ligand to the distal cluster indicate a quite extensive structural similarity between *Aquifex* I and II hydrogenases and the *Desulfovibrio gigas* proteins.

Whereas the overall sequence homology between *Aquifex* hydrogenase III and the *Desulfovibrio gigas* enzyme is significantly lower than for hydrogenases I and II, both the histidine ligand to the distal cluster and the absence of a fourth cysteine ligand to the intermediate cluster are conserved. In line with the latter sequence feature, a strong signal from a [3Fe-4S] cluster was observed in EPR spectra from both hydrogenase I and hydrogenase III from *A. aeolicus* (Fig. 3). By contrast, the first motif of cysteine ligands to the proximal cluster in *Aquifex* differs significantly from that of most other [NiFe] hydrogenases. Two adjacent cysteine residues are present in the respective sequence region of *Aquifex* hydrogenase III, whereas in almost all other [NiFe] hydrogenase small subunits, a CXXC motif is found. In fact, the sequence motif observed in *Aquifex* resembles that found in the NuoB protein from complex I, a protein sharing a common ancestry with the small subunit of [NiFe] hydrogenases (Albracht and Hedderich 2000). Two adjacent cysteines are considered to be sterically unable to ligate two iron atoms of a 4Fe-4S cluster (Ohnishi 1998). For the NuoB protein, ligation of the so-called N2 center has therefore been proposed to include a non-cysteine residue (Ahlers et al. 2000). Correspondingly, the two adjacent residues in the sequence of the hydrogenase III small subunit may not both be ligands, and an alternative (cysteine or non-cysteine) residue may be required to achieve ligation of the proximal cluster. The only available cysteine in the sequence of the N-terminal domain would be the residue 12 sequence positions upstream from the "third" ligand to the proximal cluster. In the structure of the *Desulfovibrio gigas* enzyme, this sequence position lies at the surface of the protein opposite to the proximal cluster. We therefore consider it rather unlikely that the respective cysteine in the *Aquifex* hydrogenase III can serve as a cluster ligand. Noteworthily, the alignment shown in Fig. 4 suggests that in the NuoB protein, the second cysteine of the twin pair corresponds to the second cysteine in the CXXC motif of the small subunits. By contrast, in *Aquifex* hydrogenase III, the first residue of the cys twin pair aligns with the first cys of the above-mentioned motif. This first cys in the CXXC motif is strongly exposed at the surface of the small subunit towards the interface with the large subunit, whereas the second one is fully buried. From the sequence alignment, it therefore seems likely that the exposed cluster ligand in *Aquifex* hydrogenase III is still a cysteine, whereas the buried edge of the proximal cluster is ligated by a non-cysteine residue (or a water molecule). A more in-depth EPR study of *Aquifex* hydrogenase III will yield information such as to what extent there are similarities in EPR properties between the NuoB N2-cluster and the proximal [Fe-S] center of hydrogenase III.

The N-terminal region in the small subunit of both hydrogenases I and II contains the sequence motif addressing the protein towards the periplasmic space via the twin arginine translocation system (Wu et al. 2000). These two hydrogenases from *Aquifex* are therefore periplasmic enzymes. Hydrogenase I most probably is anchored to the membrane via the membrane-integral cytochrome *b* present in the operon downstream of the large subunit, whereas hydrogenase II possibly interacts with another membrane-integral *b*-type cytochrome. Hydrogenase III, by contrast, lacks the tat-motif and therefore most likely represents a cytoplasmic hydrogenase.

Cytochrome b

The operon of *Aquifex* hydrogenase I contains a gene putatively coding for a *b*-type cytochrome in the typical order of genes in the operon (i.e., small subunit, large subunit, cytochrome). In the purification procedure, hydrogenase I was obtained in two distinct forms. One of these forms is a soluble enzyme containing only the large and small subunits. The second form was extracted from the membrane fraction by detergent treatment and was found to contain a 25-kDa protein in addition to the large and small hydrogenase subunits. Optical and EPR spectroscopy demonstrated the presence of at least two low-spin heme species with differing redox potentials. Blast searches demonstrated a strong homology of this protein to the cytochrome *b* subunit of group 1 hydrogenases from respiring proteobacteria such as *Wollinella succinogenes* (Dross et al. 1992; Gross et al. 1998; Meek and Arp 2000).

Hydrogenase II is encoded by an operon with a somewhat unusual organization. The genes for the small and large subunits are separated by two additional ORFs, the first of which is likely to code for a membrane-integral *b*-type cytochrome, whereas the second one represents an [8Fe-8S]-ferredoxin. A similar operon structure is found for the hynSL-hydrogenase (Rákhely et al. 1998; Vignais et al. 2001) from the γ-proteobacterium *Thiocapsa roseopersicina*. The sequence of the putative cytochrome *b* of the *Thiocapsa* hydrogenase has been pointed out to be related to cytochrome *b* from dissimilatory nitrate reductase and to a gene product of the dsr-locus of γ-proteobacteria, which in general codes for the sulfur-oxidizing enzyme system (Dahl et al. 1999).

Phylogenetic analysis

Unrooted phylogenetic trees were constructed from a sample of [NiFe] hydrogenases covering all major groups discussed by Vignais et al. (2001). The trees obtained on the large and small subunits were globally consistent and differed only slightly in branching topologies of three nodes. The bootstrap values for all nodes were significantly higher in the phylogram calculated on the small subunit, which is represented in Fig. 5. One of the three controversial branching topologies concerns hydrogenase III from *Aquifex*, as will be discussed below. The tree shown in Fig. 5 roughly corresponds to the previously proposed classification of [NiFe] hydrogenases into four major groups (Wu and Mandrand 1993; Vignais et al. 2001). In line with the sequence signatures of the large subunit mentioned above, hydrogenases I and II from *A. aeolicus* clearly fall into group 1 and are located among the proteobacterial counterparts.

The location of *Aquifex* hydrogenases I and II among the proteobacterial counterparts seemingly is in conflict with the phylogenetic positioning (based on 16S rRNA) of the Aquificales as the earliest diverging branch of the Bacteria. Several other enzymes from *Aquifex* have been shown to be close to proteobacterial homologues. It has therefore been proposed that the 16S rRNA positioning of the Aquificales might be in error. However, as pointed

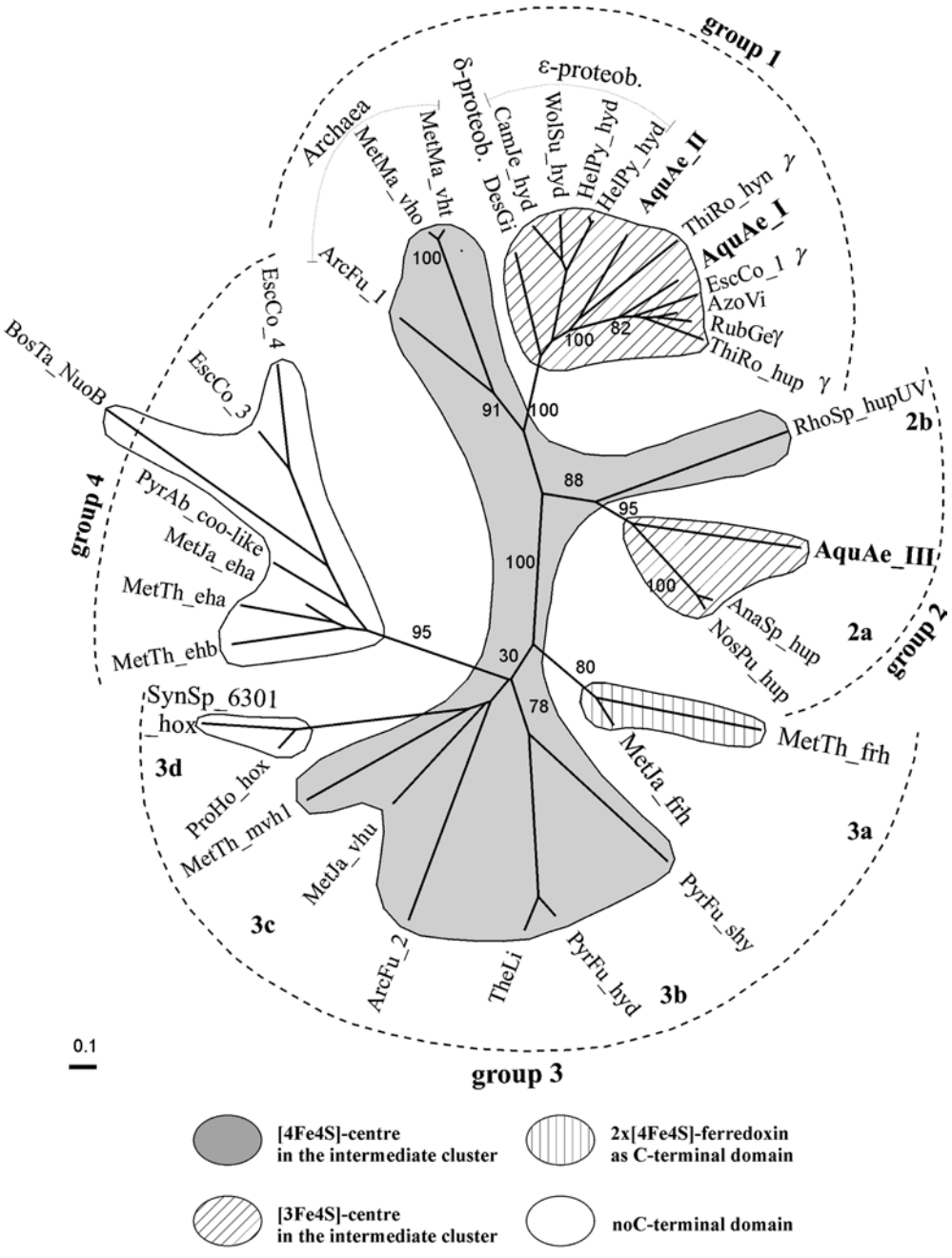

Fig. 5 Unrooted phylogenetic tree calculated from multiple sequence alignments of small subunits of [NiFe] hydrogenases. The three hydrogenases from *Aquifex* are indicated in *bold*. Attributions to the four major groups based on sequence signatures of the large subunit as defined by Wu and Mandrand (1993) are shown by *dashed arcs*. The following abbreviations for species names are used: AnaSp, *Anabaena* sp. PCC7120; ArcFu, *Archaeoglobus fulgidus*; AzoVi, *Azotobacter vinelandii*; BosTa, Bos taurus, CamJe, *Campylobacter jejuni*; DesGi, *Desulfovibrio gigas*; EscCo, *Escherichia coli*; HelPy, *Helicobacter pylori*; MetJa, *Methanococcus jannaschii*; MetMa, *Methanosarcina mazei*; MetTh, *Methanobacterium thermoautotrophicum*; NosPu, *Nostoc punctiforme*; ProHo, *Prochlorothrix hollandica*; PyrAb, *Pyrococcus abyssi*; PyrFu, *Pyrococcus furiosus*; RhoSp, *Rhodobacter sphaeroides*; RubGe, *Rubrivivax gelatinosus*; SynSp, *Synechocystis* sp. PCC6803; TheLi, *Thermococcus litoralis*; ThiRo, *Thiocapsa roseopersicina*

out previously (Schütz et al. 2000), it seems more likely to us that Aquificales have encountered rather extensive lateral gene transfer from a proteobacterial donor closely related to the ϵ-subgroup. A gene by gene analysis of the *A. aeolicus* genome has shown that about 20% of *Aquifex* ORFs are closely related to proteobacterial genes, whereas the remaining 80% correspond to the 16S rRNA positioning of this species (Brugna, unpublished). It is therefore not surprising that a whole genome comparison study confirmed the early divergence of the Aquificales (Snel et al. 1999).

Hydrogenase III, in contrast, cannot be straightforwardly attributed to one of the four major groups. The phylogram of the small subunit clusters hydrogenase III together with sensory and cyanobacterial uptake hydrogenases. As will be discussed below, the cellular abundance of the *Aquifex* hydrogenase III rules out a role as an H_2-sensing enzyme. Phylograms based on the large subunit position hydrogenase III separated from all major groups intermediate between group 2 and group 3 enzymes, albeit with lower bootstrap values (50 vs 88) for the respective nodes.

General phylogenetic inferences

The hydrogenases represented on the phylogram in Fig. 5 are coded by different shadings in order to indicate important structural parameters of the small subunits. The figure suggests that the archetypal small subunit of [NiFe] hydrogenases contained three different [4Fe-4S]-clusters. The intermediate cluster would then have been transformed into a [3Fe-3S] center twice independently in the proteobacterial region of group 1 hydrogenases and in the branch containing the cyanobacterial uptake hydrogenases and the *Aquifex* hydrogenase III. The distinct sequence features (Fig. 4) surrounding the respective position (i.e., the cysteine residue that is present when the intermediate cluster is a [4Fe-4S] center) corroborate the independence of these events. The surface-exposed histidine ligand to the distal cluster, common to all group 1 hydrogenases, is replaced by a cysteine residue in all group 3 hydrogenases and possibly in the cyanobacterial uptake hydrogenases (group 2a), where the respective ligand to the distal cluster obviously is in a position different from the bulk of [NiFe] hydrogenases.

The C-terminal domain of the small subunit appears to have been lost (or more likely replaced by an [8Fe-8S] ferredoxin) in three different places on the tree, i.e., in the group 4 enzymes, in the bi-directional hydrogenases from cyanobacteria, and in the group 3a hydrogenases. In the latter case, an [8Fe-8S] ferredoxin domain is directly fused to the N-terminal domain harboring the proximal cluster.

Group 1 certainly contains the highest number of known representatives (only a fraction of which is depicted in the tree). The group 1 subtree reflects relatively well the phylogeny of species as based on 16S rRNA sequences (Olsen et al. 1994). The archaeal species are well separated from the bacterial representatives, and the proteobacterial hydrogenases cluster in line with the taxonomic α- to γ-subgroups. As detailed above, hydrogenases I and II from *Aquifex* most probably result from lateral gene transfer.

As already mentioned by Vignais et al. (2001), the topology of the whole tree therefore suggests the presence of four distinct hydrogenases already in the common ancestor of the phylogenetic tree. Each of these four hydrogenases would then have evolved vertically and one or the other would have been lost in certain branches of the tree. Such a scenario is strongly reminiscent of what is suggested from the phylogenetic trees of the three different groups of cytochrome oxidase (Pereira et al. 2001) but is different from the situation for the cytochrome bc complexes, which seem to have existed in only one copy at the root of the tree (Schütz et al. 2000). In contrast to the latter enzyme, both cytochrome oxidase and hydrogenase have thus already diversified within the common ancestor.

In the depicted tree, the NuoB protein from complex I-type enzymes, considered to share common roots with [NiFe] hydrogenases (Albracht and Hedderich 2000), diverges from within group 4 hydrogenases. The same topology is found in phylograms of the large subunit including the NuoD protein (not shown). This is in contrast to phylograms shown by Vignais et al. (2001) but in line with results presented by Friedrich and Scheide (2000).

Conclusions

The genome of the hyperthermophilic bacterium *Aquifex aeolicus* contains genes potentially coding for three distinct [NiFe] hydrogenases. As shown above, all three hydrogenases are expressed under the growth conditions used. In line with the sequence signatures, two of these hydrogenases (hydrogenase I and II) were found to interact with the membrane, whereas hydrogenase III was observed as a soluble enzyme in the cytoplasm. Two of these hydrogenases could be further purified and characterized. Hydrogenase I was obtained in two different states, i.e., soluble and containing only the membrane-integral large and small subunits as well as complexed with cytochrome *b*. This enzyme shows all the molecular properties of group 1 hydrogenases as defined by Vignais et al. (2001). The diheme *b*-type cytochrome most likely serves as entry point into the quinone pool, as demonstrated by site-specific mutagenesis in *Wollinella succinogenes* (Gross et al. 1998) funneling the electrons towards energy-conserving electron transport enzymes and ultimately towards the terminal electron acceptors. As shown above, hydrogenase I from *Aquifex* can be isolated in a complex with membrane-integral cytochrome *b*. But, since the velocities of quinone reduction reported for the *Hydrogenobacter* (Ishii et al. 2000) enzyme (kinetic traces lasting hundreds of seconds) appear

very slow for a catalyzed electron transfer step, this reaction may be non-specific and we therefore consider the diheme *b*-type cytochrome as indispensable for electron donation to the quinone pool (see Fig. 6c).

Despite its presence in the membrane fraction, all attempts to purify hydrogenase II from *A. aeolicus* remained unsuccessful. The *b*-type cytochrome in hydrogenase II most probably plays a role analogous to that of the *b*-type heme protein of hydrogenase I, i.e., connecting the electron wire of the membrane-extrinsic small subunit's [Fe-S]-clusters to the quinone pool of the lipid phase (see Fig. 6c).

Cytochrome bc_1 complex and cytochrome oxidase have been purified (Schütz et al., ms in preparation; Baymann et al., ms in preparation) from the same batch of cell material from which the hydrogenases dealt with in this article have been obtained. It therefore seems quite likely to us that a considerable fraction of electrons delivered from hydrogenases I and II into the quinone pool pass through the cytochrome bc_1 complex and end up reducing molecular oxygen as depicted in Fig.6c.

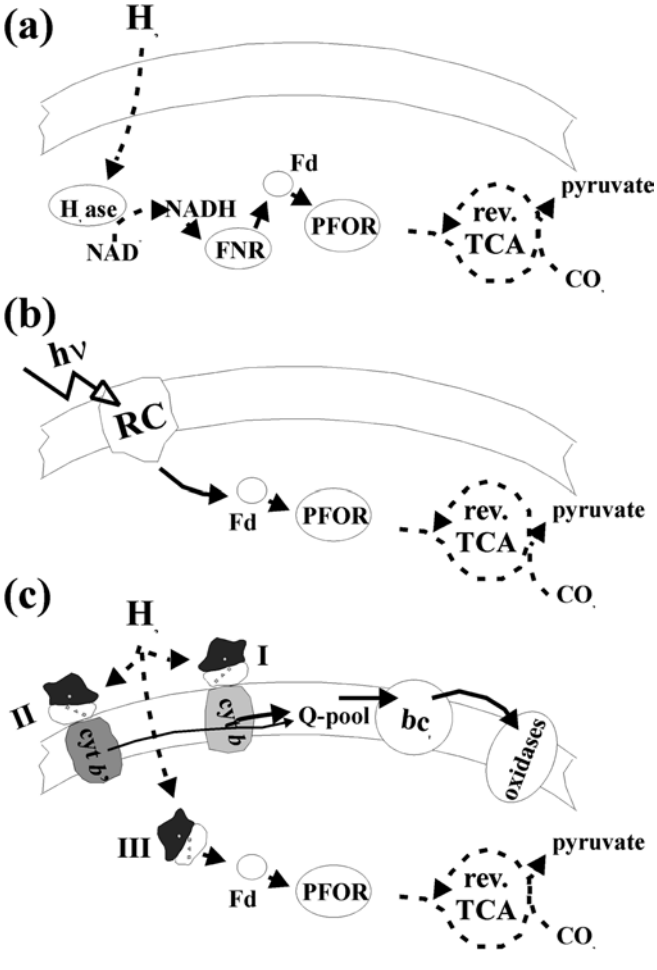

Fig. 6 Schematic representations of **a** the reaction scheme proposed by Ishii et al. (2000) for the role of hydrogen oxidation in the CO_2-fixing pathway of *H. thermophilus*, **b** the likely functioning of the reverse TCA cycle in phototrophic green sulfur bacteria (Evans et al. 1966), and **c** the proposed cellular functions of the three hydrogenases from *Aquifex aeolicus*. *Fd* Ferredoxin, *FNR* ferredoxin:NAD-oxidoreductase, *PFOR* pyruvate:ferredoxin oxidoreductase, *RC* photosynthetic reaction center

This raises the question of the difference in function between hydrogenases I and II in *Aquifex*. Clues to this question may be provided by recent work on *Thiocapsa roseopersicina* (Rákhely et al. 1998) where two distinct hydrogenases, hupSL and hynSL, are present that correspond in gene organization to *Aquifex* hydrogenases I and II, respectively. In *T. roseopersicina*, hynSL was found to be constitutively expressed, whereas hupSL was expressed only under nitrogen-fixing conditions. HupSL therefore probably oxidizes hydrogen produced "internally" during nitrogen fixation. It is tempting to consider that hydrogenases I and II in *Aquifex* might also differentially work as oxidizers of hydrogen arising from different sources. Since the enzymes of the nitrogen-fixing pathway are not found in the genome from *Aquifex aeolicus*, this specific metabolism cannot play a role in *Aquifex*. A more detailed analysis of the differential expression of hydrogenases I and II under a range of growth conditions is required to elucidate this problem.

Hydrogenase III has been isolated as a soluble cytoplasmic enzyme. The phylogram shown in Fig. 5 clusters hydrogenase III together with sensory hydrogenases and cyanobacterial uptake enzymes. A role as hydrogen sensor as proposed by Vignais et al. (2001) is very unlikely in view of the cellular abundance of hydrogenase III. Sensory hydrogenases typically are synthesized at very low levels, and/or the respective enzymes exhibit only poor hydrogenase activity (Rákhely et al. 1998; Bernhard et al. 2001). Activity levels measured on hydrogenase III, in contrast, resemble those reported for various [NiFe] hydrogenases from hyperthermophilic species (Amutha et al. 1998; Sapra et al. 2000). Cyanobacterial uptake hydrogenases have been shown to consume the molecular hydrogen produced as a byproduct of the N_2-fixing reaction sequence (Happe et al. 2000). Since N_2 fixation via nitrogenase does not occur in *Aquifex*, a respective function also seems unlikely to us.

The most probable role for hydrogenase III in *A. aeolicus* seems to be an involvement in the CO_2-fixation pathway. No gene for RubisCo is present in the genome of *A. aeolicus*, but all enzymatic activities required for the reductive TCA cycle (Evans 1966) have been demonstrated in *A. pyrophilus* (Beh 1993) and the key enzymes of this cycle are present in the *A. aeolicus* genome (Deckert et al. 1998). The presence of a number of these enzymes has furthermore been shown in *Hydrogenobacter thermophilus* (Yoon et al. 1996a, 1996b). Aquificales are therefore among the few organisms described so far to use the reductive TCA cycle as CO_2-fixing mechanism. Since the reaction of the key enzyme of this pathway, i.e., pyruvate:ferredoxin oxidoreductase (PFOR), energetically strongly favors electron transfer from pyruvate to ferredoxin, the reversal of this reaction requires a highly reduced pool of low-potential ferredoxins.

Another representative of the very limited class of species using the reductive TCA cycle for CO_2 fixation is

the green sulfur bacteria. In these organisms, a photosynthetic reaction center related to photosystem I of cyanobacteria and chloroplasts (Baymann et al. 2001) performs the light-induced reduction of low-potential electron acceptors ($E_m << -500$ mV), which transfer electrons to ferredoxin. The absence of a gene coding for Fd:NAD-reductase (FNR) in the genome of the green sulfur bacterium *Chlorobium tepidum* (TIGR, unpublished genome) indicates that the electrons from ferredoxin (Fd) are directly fed into the reverse TCA cycle via PFOR (see Fig. 6b).

The only source of highly reducing equivalents in Aquificales is electrons obtained from the oxidation of molecular hydrogen, and we therefore considered it very likely that the cytoplasmic hydrogenase III provides the reducing power driving the TCA cycle in reverse. In line with this function, hydrogenase III was found to be optimized for the reduction of low-potential electron acceptors (such as ferredoxins; see Results section). A corresponding role for hydrogen uptake has been proposed previously for *H. thermophilus* (Ishii et al. 2000). In the respective model for *Hydrogenobacter*, the electrons issued from hydrogenase are thought to reduce NAD^+ and pass via an FNR-type enzyme onto ferredoxin (as depicted in Fig. 6a). However, NADH, with its comparatively high redox midpoint potential, appears to be poorly suited to drive this reaction. Moreover, no NAD-reducing activity could be detected in any of the hydrogenases studied in our work, and the subunits responsible for NAD reduction in NADH-dependent hydrogenases (group 3d in Fig. 5) could not be detected in the *Aquifex* genome. The only genes showing significant homology to these subunits are annotated as the nuoE, nuoF, and nuoG subunits of complex I. Since the *Aquifex* complex I was recently shown to indeed oxidize NADH (Scheide et al. 2002) and therefore to require the nuoE, nuoF, and nuoG subunits, we conclude that none of the *Aquifex* hydrogenases is able to directly reduce NAD. Moreover, direct electron transfer from hydrogenases to ferredoxin has been observed in *Clostridium* species (Scheide et al. 2002; Akagi 1967), suggesting the sequence of electron transfer steps shown in Fig. 6c.

It therefore seems likely, as detailed in this figure, that the *Aquifex* hydrogenases I and II function in energy conservation, whereas hydrogenase III most probably is required for CO_2 fixation.

Acknowledgements We would like to thank Prof. T. Friedrich (Freiburg, Germany) for stimulating discussions, Dr. F. Baymann and Dr. C. Aubert (Marseille, France) for critical reading of the manuscript, as well as Dr. M. Rousset (Marseille, France) for valuable comments, D. Moinier (Protein sequencing Unit, B.I.P., Marseilles, France) for proteomic experiments, and R. Lebrun (Protein sequencing Unit, B.I.P., Marseilles, France) for performing the N-terminal sequence determination. The work of KOS was financially supported by the Fonds der Chemischen Industrie, and the project on *Aquifex* at the BIP in Marseille benefited from financial support by the PCV program of the CNRS and by the CNES.

References

Ackrell BA, Asato RN, Mower HF (1966) Multiple forms of bacterial hydrogenases. J Bacteriol 92:828–838

Adams MWW (1990) The structure and mechanism of iron-hydrogenases. Biochim Biophys Acta 1020:115–145

Adams MWW (1994) Biochemical diversity among sulfur-dependent, hyperthermophilic microorganisms. FEMS Microbiol Rev 15:261–277

Adams MWW, Kelly RM (1998) Finding and using hyperthermophilic enzymes. Trends Biotechnol 16:329–332

Ahlers PM, Zwicker K, Kerscher S, Brandt U (2000) Function of conserved acidic residues in the PSST homologue of complex I (NADH:ubiquinone oxidoreductase) from *Yarrowia lipolytica*. J Biol Chem 275:23577–23582

Akagi JM (1967) Electron carries for the phosphoroclastic reaction of *Desulfovibrio desulfuricans*. J Biol Chem 242:2478–2483

Albracht SPJ (1993) Intimate relationships of the large and the small subunits of all nickel hydrogenases with two nuclear-encoded subunits of mitochondrial NADH: ubiquinone oxidoreductase. Biochem Biophys Acta 1144:221–224

Albracht SPJ, Hedderich R (2000) Learning from hydrogenases: location of a proton pump and of a second FMN in bovine NADH–ubiquinone oxidoreductase (Complex I). FEBS Lett 485:1–6

Altschul SF, Gish W, Miller W, Myers EW, Lipman DJ (1990) Basic local alignment search tool. J Mol Biol 215:403–410

Amutha B, Khire JM, Khan MI (1998) Characterization of a novel exo-N-acetyl-beta-D-glucosaminidase from the thermotolerant *Bacillus* sp. NCIM 5120. Biochem Biophys Acta 1425:300–310

Baymann F, Tron P, Schoepp-Cothenet B, Aubert C, Bianco P, Stetter KO, Nitschke W, Schutz M (2001) Cytochromes c555 from the hyperthermophilic bacterium *Aquifex aeolicus* (VF5). 1. Characterization of two highly homologous, soluble and membranous, cytochromes c555. Biochemistry 40:13681–13689

Beh M, Strauss G, Huber R, Stetter KO, Fuchs G (1993) Enzymes of the reductive citric acid cycle in the autotrophic eubacterium *Aquifex pyrophilus* and in the archaebacterium *Thermoproteus neutrophilus*. Arch Microbiol 160:306–311

Bernhard M, Benelli B, Hochkoeppler A, Zannoni D, Friedrich B (1997) Functional and structural role of the cytochrome *b* subunit of the membrane-bound hydrogenase complex of *Alcaligenes eutrophus* H16. Eur J Biochem 248:179–186

Bernhard M, Buhrke T, Bleijlevens B, De Lacey AL, Fernandez VM, Albracht SPJ, Friedrich B (2001) The H_2 sensor of *Ralstonia eutropha*. Biochemical characteristics, spectroscopic properties, and its interaction with a histidine protein kinase. J Biol Chem 276:15592–15597

Blamey JM, Adams MWW (1993) Purification and characterization of pyruvate ferredoxin oxidoreductase from the hyperthermophilic archaeon *Pyrococcus furiosus*. Biochem Biophys Acta 1161:19–27

Blasie JK, Erecinska M, Samuels S, Leigh JS (1978) The structure of a cytochrome oxidase-lipid model membrane. Biochim Biophys Acta 501:33–52

Bradford MM (1976) A rapid and sensitive method for the quantitation of microgram quantities of protein utilizing the principle of protein-dye binding. Anal Biochem 72:248–254

Bryant FO, Adams MWW (1989) Characterization of hydrogenase from the hyperthermophilic archaebacterium, *Pyrococcus furiosus*. J Biol Chem 264:5070–5079

Cammack R, Bagyinka C, Kovacs KL (1989) Spectroscopic characterization of the nickel and iron-sulphur clusters of hydrogenase from the purple photosynthetic bacterium *Thiocapsa roseopersicina*. 1. Electron spin resonance spectroscopy. Eur J Biochem 182:363–366

Charnock JS, Cook DA, Casey R (1971) The role of cations and other factors on the apparent energy of activation of (Na + + K +)-ATPase. Arch Biochem Biophys 147:323–329

Dahl C, Rakhely G, Pott-Sperling AS, Fodor B, Takacs M, Toth A, Kraeling M, Gyorfi K, Kovacs A, Tusz J, Kovacs KL (1999)

Genes involved in hydrogen and sulfur metabolism in phototrophic sulfur bacteria. FEMS Microbiol Lett 180:317–324
Deckert G, Warren PV, Gaasterland T, Young WG, Lenox AL, Graham DE, Overbeek R, Snead MA, Keller M, Aujay M, Huber R, Feldman RA, Short JM, Olsen GJ, Swanson RV (1998) The complete genome of the hyperthermophilic bacterium *Aquifex aeolicus*. Nature 392:353–358
Dross F, Geisler V, Lenger R, Theis F, Krafft T, Fahrenholz F, Kojro E, Duchene A, Tripier D, Juvenal K, Kröger A (1992) The quinone-reactive Ni/Fe-hydrogenase of *Wolinella succinogenes*. Eur J Biochem 206:93–102
Evans MCW, Buchanan BB, Arnon DI (1966) A new ferredoxin-dependent carbon reduction cycle in a photosynthetic bacterium. Proc Natl Acad Sci USA 55:928–934
Fauque G, Peck HD, Moura JJ, Huynh BH, Berlier Y, DerVartanian DV, Teixeira M, Przybyla AE, Lespinat PA, Moura I (1988) The three classes of hydrogenases from sulfate-reducing bacteria of the genus *Desulfovibrio*. FEMS Microbiol Rev 4:299–344
Friedrich B, Schwartz E (1993) Molecular biology of hydrogen utilization in aerobic chemolithotrophs. Annu Rev Microbiol 47:351–383
Friedrich T, Scheide D (2000) The respiratory complex I of bacteria, archaea and eukarya and its module common with membrane-bound multisubunit hydrogenases. FEBS Lett 479:1–5
Gross R, Simon J, Lancaster RD, Kröger A (1998) Identification of histidine residues in *Wolinella succinogenes* hydrogenase that are essential for menaquinone reduction by H2. Mol Microbiol 30:639–646
Guigliarelli B, More C, Fournel A, Asso M, Hatchikian EC, Williams R, Cammack R, Bertrand P (1995) Structural organization of the Ni and (4Fe-4S) centers in the active form of *Desulfovibrio gigas* hydrogenase. Analysis of the magnetic interactions by electron paramagnetic resonance spectroscopy. Biochemistry 34:4781–4790
Happe T, Schutz K, Bohme H (2000) Transcriptional and mutational analysis of the uptake hydrogenase of the filamentous cyanobacterium *Anabaena variabilis* ATCC 29413. J Bacteriol 182:1624–1631
Huber R, Stetter KO (2001) Discovery of hyperthermophilic microorganisms. Methods Enzymol 330:11–24
Huber R, Huber H, Stetter K-O (2000) Towards the ecology of hyperthermophiles: biotopes, new isolation strategies and novel metabolic properties. FEMS Microbiol Rev 24:615–623
Ishii M, Takishita S, Iwasaki T, Peerapornpisal P, Yoshino J-I, Kodama T, Igarashi Y (2000) Purification and characterization of membrane-bound hydrogenase from *Hydrogenobacter thermophilus* strain TK-6, an obligately autotrophic, thermophilic, hydrogen-oxidizing bacterium. Biosci Biotechnol Biochem 64:492–502
Jensen ON, Larsen MR, Roepstorff P (1998) Mass spectrometric identification and microcharacterization of proteins from electrophoretic gels: strategies and applications. Proteins 2:74–89
Kelly RM, Adams MWW (1994) Metabolism in hyperthermophilic microorganisms. Antonie V. Leeuwenhoek 66:247–270
Ma K, Weiss R, Adams MWW (2000) Characterization of hydrogenase II from the hyperthermophilic archaeon *Pyrococcus furiosus* and assessment of its role in sulfur reduction. J Bacteriol 182:1864–1871
Meek L, Arp DJ (2000) The hydrogenase cytochrome *b* heme ligands of *Azotobacter vinelandii* are required for full H(2) oxidation capability. J Bacteriol 182:3429–3436
Ohnishi T (1998) Iron-sulfur clusters/semiquinones in complex I. Biochim Biophys Acta 1364:186–206
Olsen GJ (1994) Microbial ecology. Archaea, Archaea, everywhere. Nature 371:657–658
Olsen GJ, Woese CR, Overbeek R (1994) The winds of (evolutionary) change: breathing new life into microbiology. J Bacteriol 176:1–6
Pereira MM, Santana M, Teixeira M (2001) A novel scenario for the evolution of haem-copper oxygen reductases. Biochim Biophys Acta 1505:185–208
Pihl TD, Maier RJ (1991) Purification and characterization of the hydrogen uptake hydrogenase from the hyperthermophilic archaebacterium *Pyrodictium brockii*. J Bacteriol 173:1839–1844
Rákhely G, Colbeau A, Garin J, Vignais PM, Kovács KL (1998) Unusual organization of the genes coding for HydSL, the stable [NiFe]hydrogenase in the photosynthetic bacterium *Thiocapsa roseopersicina* BBS. J Bacteriol 180:1460–1465
Rutherford AWR, Sétif P (1990) Orientation of P700, the primary electron donor of photosystem I. Biochim Biophys Acta 1019:128–132
Sambrook J, Fritsch EF, Maniatis T (1989) Molecular cloning: a laboratory manual, 2nd edn. Cold Spring Harbor Laboratory Press, Cold Spring Harbor, N.Y., pp 18.60–18.75
Sapra R, Verhagen MFJM, Adams MWW (2000) Purification and characterization of a membrane-bound hydrogenase from the hyperthermophilic archaeon *Pyrococcus furiosus*. J Bacteriol 182:3423–3428
Scheide D, Huber R, Friedrich T (2002) The proton-pumping NADH:ubiquinone oxidoreductase (complex I) of *Aquifex aeolicus*. FEBS Lett 512:80–84
Schütz M, Brugna M, Lebrun E, Baymann F, Huber R, Stetter KO, Hauska G, Toci R, Lemesle-Meunier D, Tron P, Schmidt C, Nitschke W (2000) Early evolution of cytochrome *bc* complexes. J Mol Biol 300:663–675
Segel IK (1993) Enzyme kinetics. Behaviour and analysis of rapid equilibrium and steady state enzyme systems. Wiley Classics Library Edition, New York
Snel B, Bork P, Huynen MA (1999) Genome phylogeny based on gene content. Nat Genet 21:108–110
Spies M, Kil Y, Masui R, Kujo C, Ohshima T, Kuramitsu S, Lanzov V (2000) The RadA protein from a hyperthermophilic archaeon *Pyrobaculum islandicum* is a DNA-dependent ATPase that exhibits two disparate catalytic modes, with a transition temperature at 75 degrees C. Eur J Biochem 267:1125–1137
Stetter KO (1996) Hyperthermophilic procaryotes. FEMS Microbiol Rev 18:149–158
Stetter KO (1999) Extremophiles and their adaptation to hot environments. FEBS Lett 452:22–25
Surerus KK, Chen M, van der Zwaan JW, Rusnak FM, Kolk M, Duin E, Albracht SP, Münck E (1994) Further characterization of the spin coupling observed in oxidized hydrogenase from *Chromatium vinosum*. A Mossbauer and multifrequency EPR study. Biochemistry 33:4980–4993
Vignais PM, Billoud B, Meyer J (2001) Classification and phylogeny of hydrogenases. FEMS Microbiol Rev 25:455–501
Volbeda A, Charon MH, Piras C, Hatchikian EC, Frey M, Fontecilla-Camps JC (1995) Crystal structure of the nickel-iron hydrogenase from *Desulfovibrio gigas*. Nature 373:580–587
Voordouw G (1993) Molecular biology of the sulfate-reducing bacteria. In: Odom JM, Singleton RJ (eds) The sulfate-reducing bacteria: contemporary perspectives. Spinger, Berlin Heidelberg New York, pp 88–130
Wu LF, Mandrand MA (1993) Microbial hydrogenases: primary structure, classification, signatures and phylogeny. FEMS Microbiol Rev 104:243–270
Wu LF, Chanal A, Rodrigue A (2000) Membrane targeting and translocation of bacterial hydrogenases. Arch Microbiol 173:319–324
Yoon K-S, Ishi M, Igarashi Y, Kodama T (1996a) Purification and characterization of 2-oxoglutarate:ferredoxin oxidoreductase from a thermophilic, obligately chemolithoautotrophic bacterium, *Hydrogenobacter thermophilus* TK-6. J Bacteriol 178:3365–3368
Yoon K-S, Ueda Y, Ishi M, Igarashi YK, Kodama T (1996b) NADH:ferredoxin reductase and NAD-reducing hydrogenase activities in *Hydrogenobacter thermophilus* strain TK-6. FEMS Microbiol Lett 139:139–142